LA-UR-19-28448
Approved for public release; distribution is unlimited.

Title: Thermoelasticity Model for Niobium

Author(s): Burakovsky, Leonid
Baty, Samuel R.
Preston, Dean Laverne
Sjue, Sky K.
Luscher, Darby Jon

Intended for: Report

Issued: 2019-08-21

Thermoelasticity Model for Niobium

S.R. Baty[1], L. Burakovsky[2], D.L. Preston[3], S.K. Sjue[4], and D.J. Luscher[2]

[1] *Analytics Intelligence and Technology,*

[2] *Theoretical Division,*

[3] *Applied Physics Division,*

[4] *Physics Division,*

Los Alamos National Laboratory,

Los Alamos, New Mexico 87545, USA

PACS numbers:

Nb as a polymorphic material

Niobium is a polymorphic (multi-phase) material. Its phase diagram contains two experimentally confirmed solid phases, body-centered cubic (bcc) and orthorhombic Pnma, and is shown in Figs. 1 and 2. The bcc–Pnma phase boundary was determined in a recent work [1] that combines experimental study by Errandonea *et al.* using laser-heated diamond anvil cell (DAC) and the theoretical calculation of the total free energies of both solid structures using the temperature dependent effective potential (TDEP) method which takes into account anharmonic lattice vibrations.

The results of our *ab initio* quantum molecular dynamics (QMD) simulations on the melting curves of bcc-Nb and Pnma-Nb are summarized in Tables 1 and 2, respectively.

lattice constant (Å)	density (g/cm^3)	P_m (GPa)	T_m (K)
3.445	7.547	-7.9	2400
3.225	9.199	27.0	3460
3.050	10.88	79.9	4330
2.955	11.96	124	4820
2.850	13.33	191	5390
2.745	14.92	287	6050

Table 1. The six *ab initio* melting points of bcc-Nb, (P_m, T_m), obtained from the Z method implemented with VASP.

lattice constant (Å)	density (g/cm^3)	P_m (GPa)	T_m (K)
4.6215	8.696	6.5	2970
4.3910	10.14	40.1	3890
4.2450	11.22	76.4	4550
4.1145	12.32	125	5240
4.0100	13.31	180	5850
3.9160	14.29	245	6430

Table 2. The six *ab initio* melting points of Pnma-Nb, (P_m, T_m), obtained from the Z method implemented with VASP.

Figs. 3 and 4 demonstrate the time evolution of T and P, respectively, in the Z-method runs of the bcc-Nb melting point $(P, T) = (124, 4820)$. Figs. 5 and 6 demonstrate the same for the Pnma-Nb melting point $(125, 5240)$. These two points are chosen as examples and are shown in Fig. 2 as green and red diamonds, respectively. The detailed description of the Z method implemented with VASP can be found in Ref. [2].

The best fit to the six bcc-Nb datapoints gives the melting curve of bcc-Nb in the Simon-Glatzel form:

$$T_m(P) = 2750 \left(1 + \frac{P}{22.6}\right)^{0.30}, \tag{1}$$

Similarly, the best fit to the six Pnma-Nb datapoints gives the melting curve of Pnma-Nb:

$$T_m(P) = 2710 \left(1 + \frac{P}{21.0}\right)^{0.34}. \tag{2}$$

The initial slope of the bcc-Nb melting curve (1), $dT_m(P)/dP = 36.5$ K/GPa at $P = 0$, is in excellent agreement with 36 K/GPa from isobaric-heating measurements [3]. Other, theoretical value for this slope, 37.7 K/GPa [4], is in the same ballpark.

The two melting curves cross each other at (P in GPa, T in K) $(P, T) = (5.9, 2949)$ which is the bcc-Pnma-liquid triple point. The analytic form of the bcc-Pnma solid-solid phase transition boundary is assumed to be the best fit to the four theoretical transition points determined using the TDEP method, $(P, T) = (155, 3623)$, $(215, 3942)$, $(295, 4448)$, and $(395, 5141)$. Interstingly enough, the best quadratic fit to the four (P, T) points crosses the triple point determined above from independent calculation:

$$T(P) = 2946.8 + 3.8\,(P - 5.9) + 4.7 \cdot 10^{-3}\,(P - 5.9)^2,$$

or else,

$$T(P) = 2949 + 3.8\,(P - 6.48) + 4.7 \cdot 10^{-3}\,(P - 6.48)^2.$$

In what follows, we adopt the triple point to be $(6, 2950)$ and the bcc-Pnma phase boundary

$$T(P) = 2950 + 3.8\,(P - 6) + 4.7 \cdot 10^{-3}\,(P - 6)^2. \tag{3}$$

The four bcc-Pnma transition points and the phase boundary are shown in Fig. 1.

The Nb principal Hugoniot in the P-T coordinates calculated theoretically, $T(P) = 293 + 0.22\,P^{1.93}$, crosses the bcc-Pnma transition boundary at 145.3 GPa which is in agreement with experimental data on shock compression from the Russian Shock Wave

Database [5]. Indeed, assume that the bcc and Pnma portions of the Nb Hugoniot are described by straight segments $U_s = a + b\,U_p$. Then $a = \sqrt{B_0/\rho_0}$ and $b = (1 + B_0')/4$ [6]. The two sets of values for both bcc-Nb and Pnma-Nb come from the corresponding equations of state (EOS) in the third-order Birch-Murnaghan form,

$$P(\rho) = \frac{3}{2}\,B_0\left(\eta^{7/3} - \eta^{5/3}\right)\left[1 + \frac{3}{4}(B_0' - 4)\left(\eta^{2/3} - 1\right)\right],$$

where $\eta = \rho/\rho_0$, and are (ρ_0 in g/cc and B_0 in GPa)

$$\mathrm{bcc - Nb:}\quad \rho_0 = 8.5696,\ \ B_0 = 170.5,\ \ B_0' = 3.85,$$

$$\mathrm{Pnma - Nb:}\quad \rho_0 = 8.5717,\ \ B_0 = 137.2,\ \ B_0' = 4.65.$$

The two equations of state are shown in Figs. 5 and 6. Note that our value of ρ_0 for bcc-Nb is identical to the Nb experimental ambient density. Our set of (B_0, B_0') for bcc-Nb is consistent with similar sets that can be found in the literature: $(168.8, 3.73)$ [7], $(168(4), 3.4(3))$ [8], $(169, 4.08)$ [9].

Fig. 7 compares the experimental Hugoniot data on $(U_s - U_p)$ vs. U_p to the combination of the two straight segments described by $a + (b-1)U_p$ with the corresponding values of a and b for the two solid phases of Nb that come from the above formulas and sets of values. Here $(U_s - U_p)$ is chosen instead of U_s to illustrate a change in compressibility, since on the Hugoniot $U_s/(U_s - U_p) = \rho/\rho_0$ [6]. The two segments are $U_s = 4.4605 + 0.2125\,U_p$ and $U_s = 4.0008 + 0.4125\,U_p$. Agreement between the data and the two segments is excellent. The segments cross each other at $U_p = 2.2985 \approx 2.3$ km/s. According to [5], along the Nb Hugoniot $P(U_p) = 39.0\,U_p + 10.3\,U_p^2$; hence, at the transition point $P(U_p = 2.3) = 144.2$ GPa, consistnet with 145.3 GPa where the Hugoniot crosses the bcc-Pnma phase boundary. Thus, the bcc-Pnma Hugoniot transition point is at ~ 145 GPa. Melting on the Hugoniot occurs at ~ 200 GPa, where the Hugoniot crosses the Pnma-Nb melting curve, as seen in Fig. 1.

The modification of the unified analytic melt-shear model

For a polymorphic material, such as Nb, the unified analytic melt-shear model describes both cold ($T = 0$) shear modulus, G, and melting temperature, T_m, as functions of

density, ρ :

$$\frac{d\ln G(\rho)}{d\ln \rho} \equiv 2\,\gamma_G(\rho) + \frac{1}{3}, \tag{4}$$

$$\frac{d\ln T_m(\rho)}{d\ln \rho} \equiv 2\,\gamma_{T_m}(\rho) - \frac{2}{3}, \tag{5}$$

where $\gamma_G(\rho)$ and $\gamma_{T_m}(\rho)$ are the corresponding Grüneisen parameters given by

$$\gamma_G(\rho) = \frac{1}{2} + \frac{\gamma_1}{\rho^{1/3}} + \frac{\gamma_2}{\rho^{q_2}}, \tag{6}$$

$$\gamma_{T_m}(\rho) = \frac{1}{2} + \frac{\gamma_1}{\rho^{1/3}} + \frac{\gamma_3}{\rho^{q_3}}, \tag{7}$$

where $\gamma_1 = \frac{7}{40}\,Z^{2/3}$, Z being the atomic number of the material.

With (3) and (4), the solutions to (1) and (2) are

$$G(\rho) = G(\rho_0)\left(\frac{\rho}{\rho_0}\right)^{4/3} \exp\left\{6\gamma_1\left(\frac{1}{\rho_0^{1/3}} - \frac{1}{\rho^{1/3}}\right) + \frac{2\gamma_2}{q_2}\,\left(\frac{1}{\rho_0^{q_2}} - \frac{1}{\rho^{q_2}}\right)\right\}, \tag{8}$$

$$T_m(\rho) = T_m(\rho_m)\left(\frac{\rho}{\rho_m}\right)^{1/3} \exp\left\{6\gamma_1\left(\frac{1}{\rho_m^{1/3}} - \frac{1}{\rho^{1/3}}\right) + \frac{2\gamma_3}{q_3}\,\left(\frac{1}{\rho_m^{q_3}} - \frac{1}{\rho^{q_3}}\right)\right\}, \tag{9}$$

where ρ_0 and ρ_m are the corresponding initial densities usually taken as those at ambient pressure (P). For a polymorphic material, these equations should be understood as the envelopes of the individual $G(\rho)$ and $T_m(\rho)$ for each of the stable solid phases of the material.

Model parameters for Nb

The values of γ_1, γ_2, q_2 and γ_3, q_3 are calculated based on the following input for bcc-Nb:

$$Z = 41, \quad A = 92.90637, \qquad \rho_0 = 8.62 \text{ g/cc} \quad \rho_m = 7.99 \text{ g/cc}$$

$$G(\rho_0) = 40.5 \text{ GPa} \quad T_m(\rho_m) = 2750 \text{ K}$$

$$\gamma_G(\rho_0) = 0.6 \;\; (\text{from the low} - \text{density data on } G = G(\rho))$$

$$\gamma_{T_m}(\rho_m) = 1.1 \;\; (\text{from the initial slope of the melting curve } T_m = T_m(\rho))$$

The values are: $\gamma_1 = 7/40\,Z^{2/3}$ [10] $= 2.08079$,

$$q_2 = 6.3, \quad \gamma_2 = -7.2 \cdot 10^5, \;\; \text{and} \;\; q_3 = 0.6, \;\; \gamma_3 = -1.54.$$

The modification of the unified melt-shear model for a polymorphic material, applied here to Nb, is described in detail in our previous work on Mo [10].

Comparison to data

Fig. 8 compares the shear modulus of Nb, described in terms of the corresponding (γ_1, γ_2, q_2) parameters from the previous section, to the results of QMD simulations (mentioned in the figure caption) on the bcc-Nb, including our own QMD results using VASP.

Fig. 9 compares the melting curve of Nb, described in terms of the corresponding (γ_1, γ_3, q_3) parameters from the previous section, to our QMD simulations using VASP. This theoretical melting curve in the P-T coordinates is shown in Fig. 1.

Thermoelastic softening parameter

In the Preston-Wallace thermoelasticity model [11]

$$G(\rho, T) = G(\rho, 0)\left(1 - \beta\,\frac{T}{T_m(\rho)}\right), \tag{10}$$

where the thermoelastic softening parameter β can in principle be a function of density. Using the exprimental data on $G(\rho_0, 0) = 40.5$ GPa [12] and $G(\rho_m, T_m(P = 0)) \approx 33.1$ GPa [13], we find

$$\beta = 0.115 \tag{11}$$

which is a half of the "canonical" value of 0.23 discussed in [11].

[1] D. Errandonea *et al.,* Niobium at high pressure and high temperature: Combined experimental and theoretical study; *submitted*

[2] L. Burakovsky, N. Burakovsky, and D.L. Preston, Phys. Rev. B **92**, 174105 (2015)

[3] J.W. Shaner, G.R. Gathers, and C. Minichino, High Temp. - High Press. **8**, 425 (1976)

[4] T. Górecki, Z. Metallkde. **68**, 231 (1977), High Temp. - High Press. **11**, 683 (1979)

[5] Russian Shock Wave Database; http://www.ihed.ras.ru/rusbank/

[6] J.D. Johnson, AIP Conference Proceedings, **429**, 27 (1998)

[7] R.G. McQueen, S.P. Marsh, J.W. Taylor, J.N. Fritz, and W.J. Carter, in *High Velocity Impact Phenomena,* edited by R. Kinslow (Academic Press, New York, 1970), p. 293

[8] T. Kenichi and A.K. Singh, Phys. Rev. B **73**, 224119 (2006)

[9] K.W. Katahara, M.H. Manghnani, and E.S. Fisher, J. Appl. Phys. **47,** 434 (1976)

[10] L. Burakovsky, D.L. Preston, S.K. Sjue, and D.E. Vaughan, Crystals **9**, 86 (2019)

[11] D.L. Preston and D.C. Wallace, Solid State Comm. **81**, 277 (1992)

[12] K.J. Carroll, J. Appl. Phys. **36**, 3689 (1965), and references therein

[13] Y. Talmor, E. Walker, and S. Steinemann, Solid State Comm. **23**, 649 (1977)

[14] P.F. Weck *et al.,* J. Appl. Phys. **125**, 245905 (2019)

[15] S.P. Kramynin and E.N. Akhmedov, J. Phys. Chem. Solids **153**, 109108 (2019)

[16] A.V. Lugovskoy, The first principles study of the phase stability and elastic properties of transition metals at ultrahigh pressures, PhD thesis; National Research Technological University "MISiS," Moscow, 2015

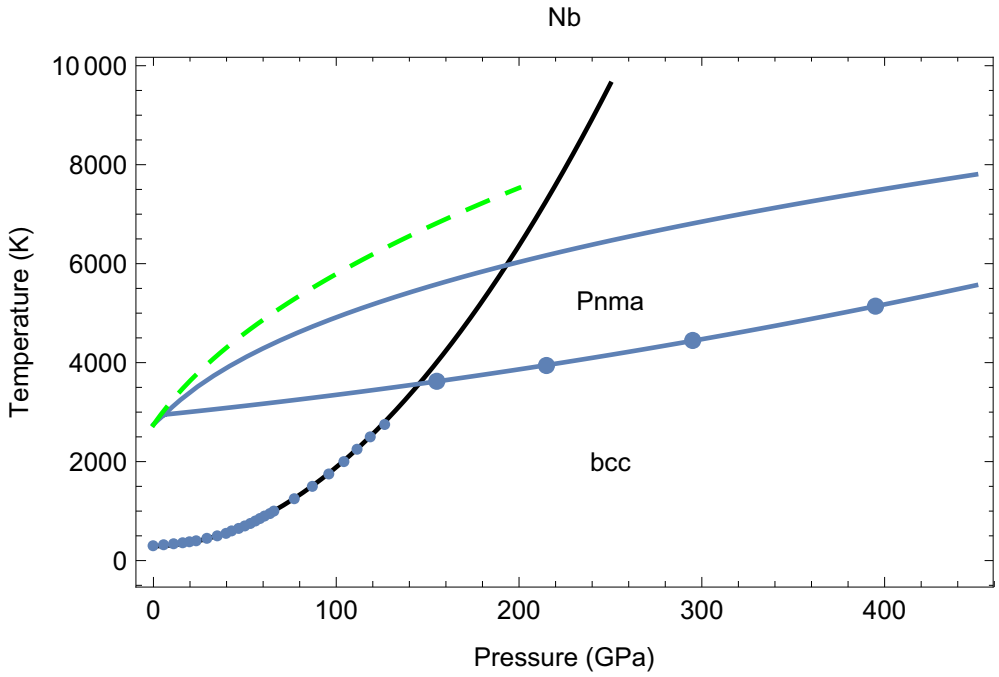

FIG. 1: The *ab initio* phase diagram of Nb. The theoretical Hugoniot points of Ref. [14] are shown for comparison with our Hugoniot (black line). The melting curve of Ref. [15] obtained from classical molecular dynamics is shown as well (green dashed lkine).

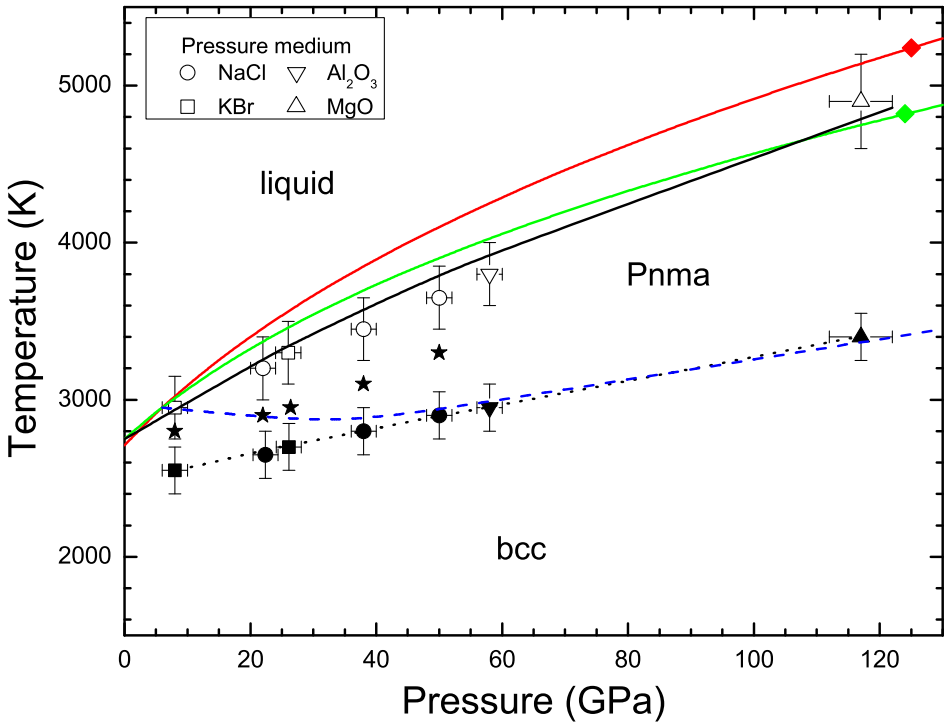

FIG. 2: The low-pressure portion of Figure 1 including the experimental results of Ref. [1]. Different symbols correspond to experiments done using different pressure media (see inset). Black solid symbols and black dotted line: the onset of recrystallization. Black empty symbols: the onset of melting. Black solid line: the Simon-Glatzel fit to the experimental melting points, $T_m(P) = 2750\,(1 + P/48)^{0.45}$ shown for comparison with the theoretical melting curve. For this fit, the initial slope, 25.8 K/GPa, is essentially lower than 36 K/GPa from isobaric heating measurements. Green and red lines: the QMD melting curves of bcc-Nb and Pnma-Nb, respectively. The initial slope of the theoretical bcc-Nb melting curve is 36.5 K/GPa. Black stars are the P-T points where the Pnma structure is detected in experiment. Error bars of these points (not shown for the sake of clarity) are comparable to those of melting and recrystallization. Blue dashed line: the theoretical bcc-Pnma phase boundary from this work.

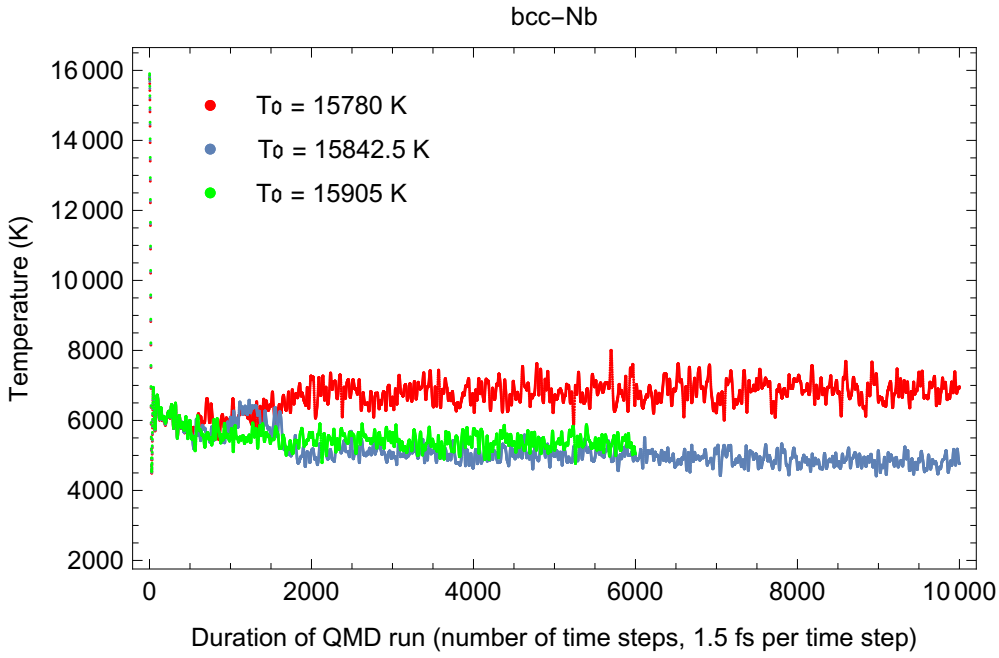

FIG. 3: The melting point of bcc-Nb at a density of 11.96 g/cc: melting T from *ab initio* Z method implemented with VASP.

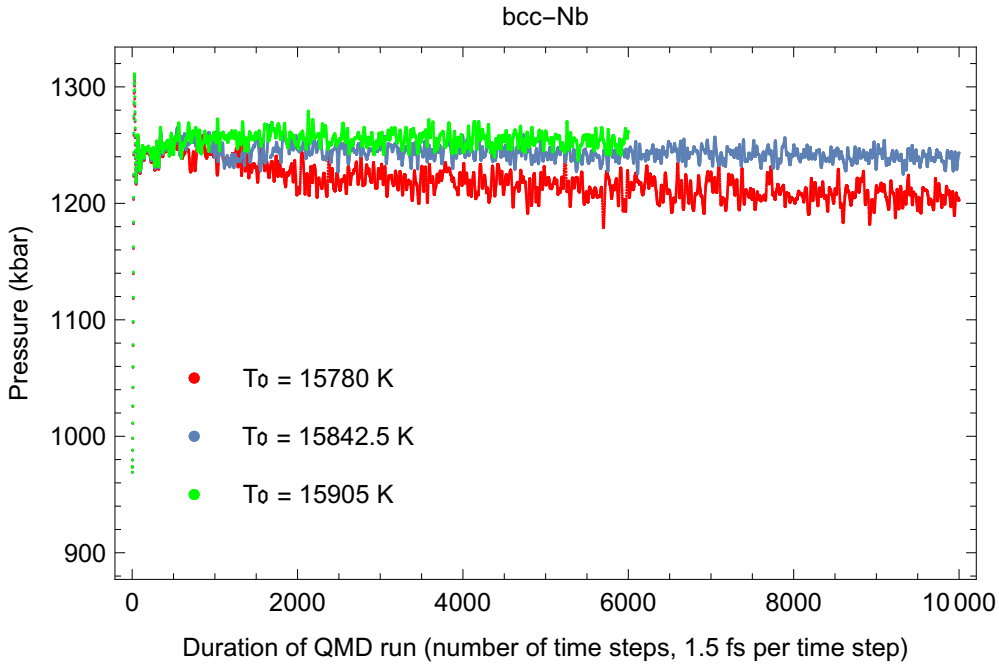

FIG. 4: The same as in Fig. 3 for melting P.

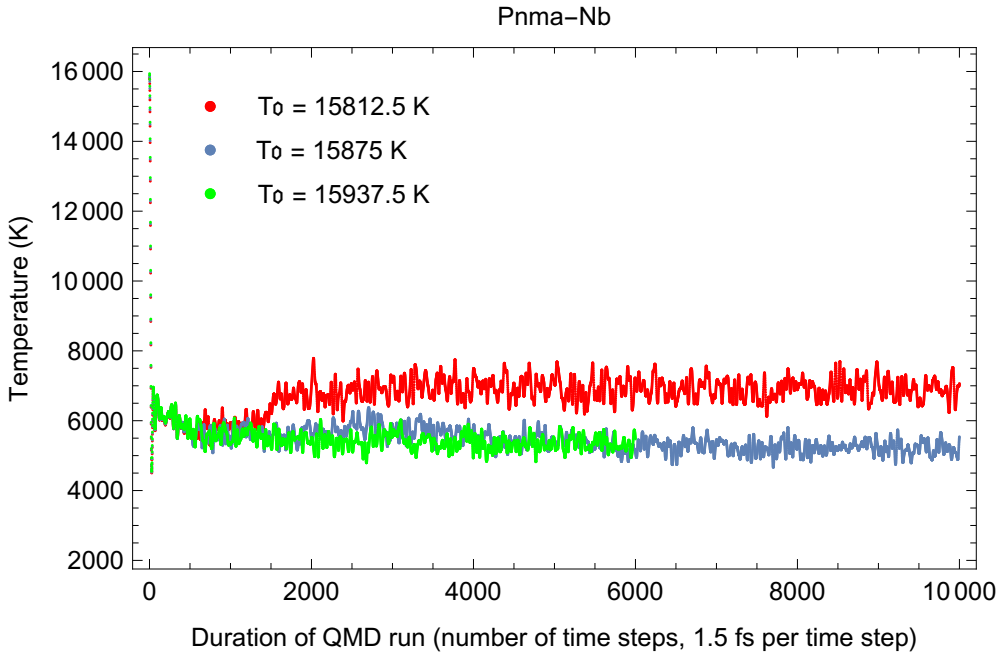

FIG. 5: The melting point of Pnma-Nb at a density of 12.32 g/cc: melting T from *ab initio* Z method implemented with VASP.

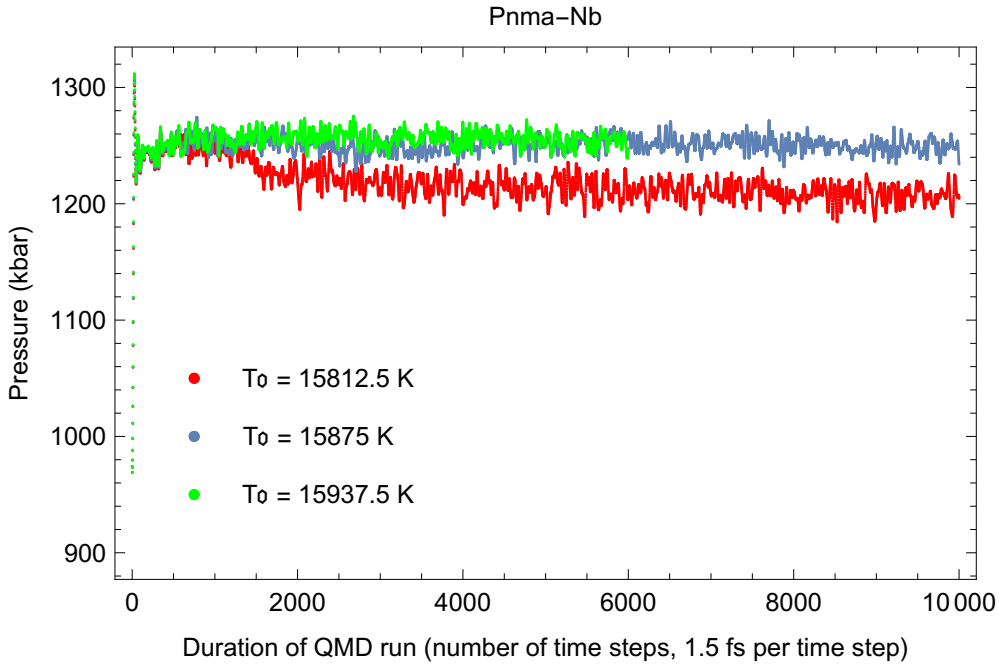

FIG. 6: The same as in Fig. 5 for melting P.

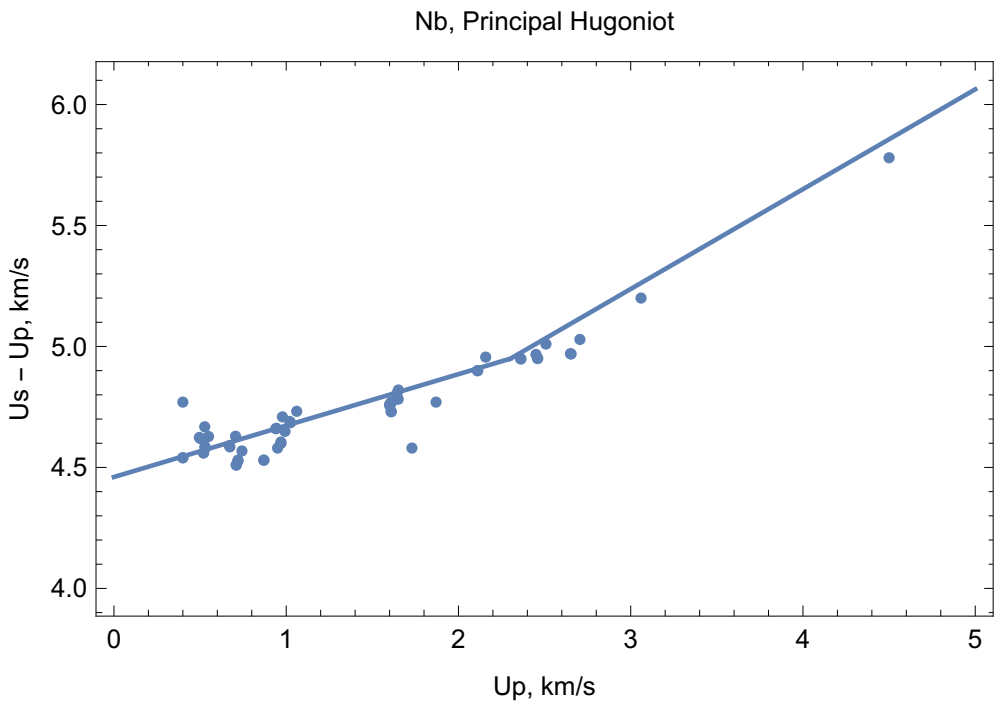

FIG. 7: $U_s - U_p$ vs. U_p along the Nb Hugoniot. Two straight segments are those of bcc-Nb (the lower one) and Pnma-Nb (the upper one) described by $U_s = a + (b-1)U_p$ with the corresponding sets of (a, b) parameters.

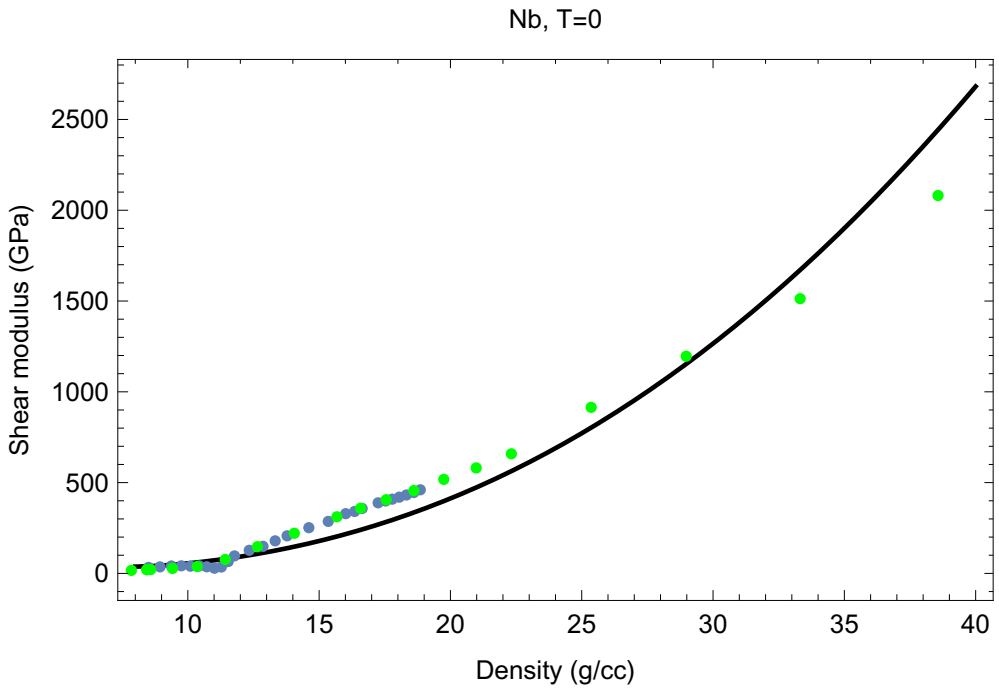

FIG. 8: The cold ($T = 0$) shear modulus of bcc-Nb: unified analytic melt-shear model (curve) vs. QMD simulations using VASP (green points). The results of QMD simulations of Ref. [16] (blue points) are also shown for comparison.

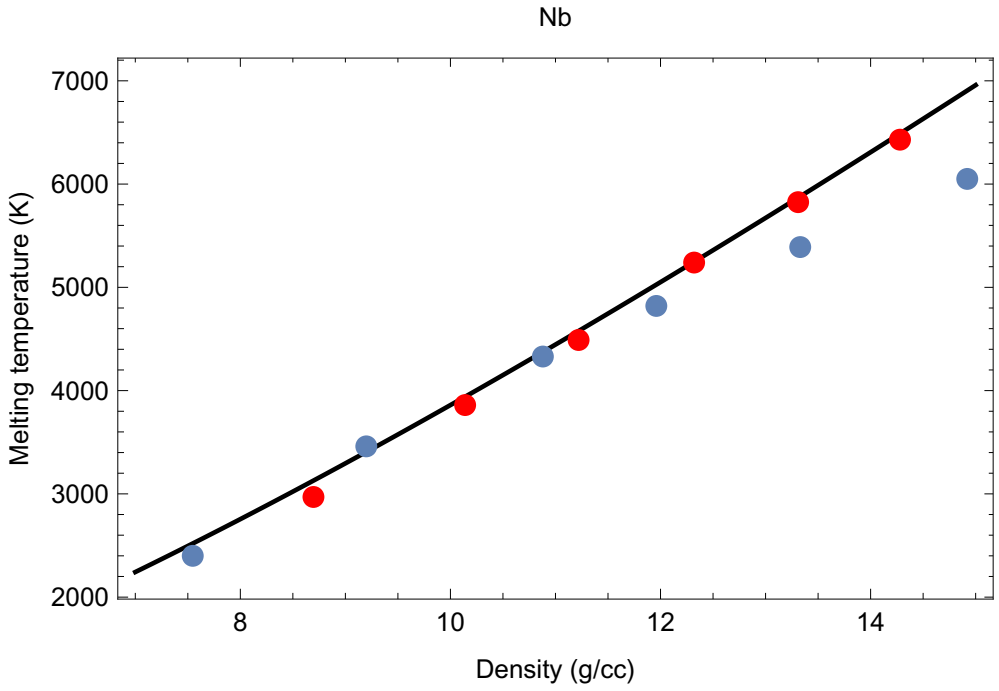

FIG. 9: The melting curve of Nb: unified analytic melt-shear model (curve) vs. QMD simulations using VASP (bcc-Nb: blue points, Pnma-Nb: red points).